THE BEHAVIOR OF COMPOSITE THIN-WALLED STRUCTURES IN DYNAMIC BUCKLING UNDER IMPACT

J. Ari-Gur* and J. Singer**
Department of Aeronautical Engineering
Technion - Israel Institute of Technology
Haifa, Israel

and

H. Röhrle***
Dornier GmbH
Friedrichshafen, FRG

Abstract

The influence of material properties, and in particular those of composites, on response and behaviour of columns under axial impact is studied. An extensive experimental investigation has been carried out on specimens made of graphite/epoxy, glass/epoxy and Kevlar/epoxy laminates with different layups. Dynamic buckling and failure are compared with those of metal columns and the relative advantages and disadvantages of the composite materials are discussed. In general, composite columns show improved dynamic buckling properties, and, with several exceptions, they may replace metal ones efficiently and reliably.

I. Introduction

Dynamic buckling of slender columns has been extensively investigated during recent years in the Aircraft Structures Laboratory at the Department of Aeronautical Engineering, Technion[1-6]. Previous studies on the response of columns to impulsive compression, reviewed in the Introduction of[1], did not treat the problem of stability limit and initiation of buckling. The definition of critical dynamic loads, that was adopted successfully in[1] and in later studies, enabled presentation of stability bounds. It was shown theoretically and experimentally that dynamic buckling loads exceed those of static loading. The Dynamic Load amplification Factor (DLF), which is the ratio of dynamic to static buckling loads, increases with the slenderness ratio of the column and decreases when the duration of impulse or the magnitude of initial geometrical imperfection are increased. In the linear elastic range material properties do not significantly affect the dynamic buckling behavior, hence dynamic buckling tests on columns of different materials yielded elastic buckling results within the same scatter. The postbuckling behavior however strongly depends on material properties.

The objectives of the present investigation are to test the validity of the conclusions on a wide range of commonly employed composite materials, identify exceptions, study the post-buckling behavior and failure modes of the various materials and propose recommendations for their efficient use.

II. Test Specimens

81 laminated composite specimens, manufactured by Dornier GmbH, and 12 2024-T3 aluminum alloy specimens were tested. Fibers of 3 different materials, all embeddedin an epoxy matrix, were used for the composite laminates: graphite HT/T300 (Torey), E-glass (Gevetex) and Kevlar (Dupont), identified in the paper by the letters C, G and K, respectively. For each material, three different symmetrical layups were produced: U-unidirectional (0°), S-"shear"laminate (±45°) and M-"mixed" (0°, ± 45°, 90°). The graphite/epoxy (C) specimens were made in 5 lengths, but the glass/epoxy (G) and Kevlar/epoxy (K) columns only in 2 lengths. Three identical specimens were made for each type. The dimensions and details of layup of the columns are presented in Appendix A of[7].

The plates from which the columns were cut were inspected by X-ray and ultrasonic methods to ascertain the quality of the laminates. The manufacture, quality control and material tests are described in[8].

The average thicknesses t (average of measurements at 4 sections) of the columns are given in Table 1, classified according to type of laminate.

TABLE 2 - MEASURED THICKNESSES OF SPECIMENS (nominally 2 mm).

	"Mixed"(M)	"Shear"(S)	Unidirect-ional (U)
Kevlar(K)	2.05mm	1.85mm	1.75mm
Graphite(C)	2.10mm	2.10mm	2.00mm
Glass(G)	2.15mm	2.25mm	2.20mm

Static tests were carried out to verify the computed coefficients of elastic stiffness A_{11} and D_{11}. The moduli A_{11} were measured in a tension test and D_{11} in a four-loading-points pure bending test. The radii of gyration were then calculated with Eq. (1)

$$r = \frac{D_{11}}{A_{11}} \qquad (1)$$

---

* Research Fellow
** L. Shirley Tark Professor of Aircraft Structures
*** Abteilungsleiter, Strukturdynamik und Sondergebiete der Strukturmechanik

and the results are presented in Table 2.

The longitudinal stiffnesses of all the glass/epoxy specimens are 11% - 14% below the computed ones. The results for the graphite/expoxy CU and CM specimens agree well with the computed A_{11}, but that for the "shear" laminate CS is 56% lower. The largest differences are obtained for the Kevlar/epoxy specimens. The measured A_{11} for the "mixed" KM and the unidirectional KU laminates are 25% and 29%, respectively, below the calculated ones. The worst combination is the KS laminate (77% lower).

TABLE 2 - STATIC TEST RESULTS
(nominal and tested)

Material	A_{11}[kN/mm]		r[mm]		$\frac{r\sqrt{12}}{t}$	
	nom.	test	nom.	test	nom.	test
CU	252	241.6	.576	.57	1.00	.99
GU	94.2	82.4	.576	.61	1.00	.96
KU	162	115.4	.576	.48	1.00	.95
CM	135	137	.635	.62	1.10	1.02
GM	58.1	51.6	.618	.65	1.07	1.05
KM	87.1	65.5	.634	.64	1.10	1.08
CS	77.6	34.0	.576	.60	1.00	.99
GS	38.8	33.3	.576	.65	1.00	1.00
KS	50.3	11.7	.576	.55	1.00	1.03

NOTE: A_{11} was measured in tension

The bending moduli D_{11} showed similar trends in the differences between measured and computed values. Hence the values of r agree fairly well and those for (r/t) show even better agreement, with a maximum 8% difference between tested and calculated values.

The width of all the specimens is b = 19mm, and the aluminum alloy columns have a thickness t = 1.6 mm.

III. Impact Tests

The test system and procedure were described in detail in[1], but are recapitulated here briefly for convenience of the reader. The specimen is positioned and clamped under a vertical tube in which a striking mass is dropped on the column. Impact tests are carried out with increasing velocity, and in each test the striking velocity is measured and the outputs of a pair of strain gages, bonded on both faces of the thin column, are recorded. The strain records, stored in the magnetic memories of high frequency digital recorders, are then simultaneously plotted on a multichannel pen-recorder together with their sum and difference which are the axial strain (ϵ_c) and bending strain (ϵ_b), respectively multiplied by two.

For each specimen a bending-compression curve (see for example Fig. 1) is then plotted.

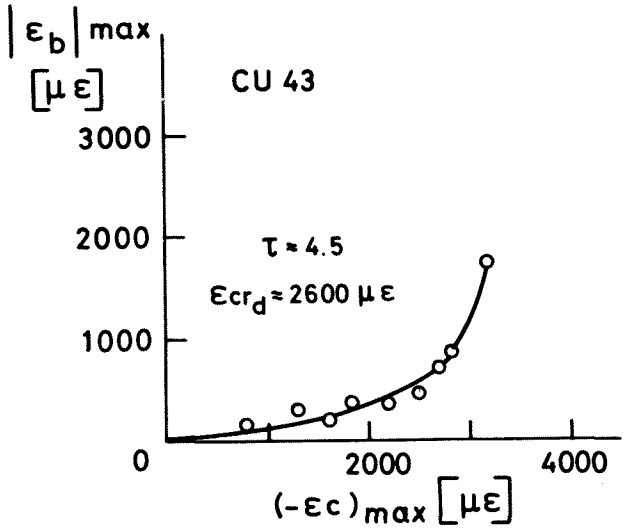

Figure 1. Bending-compression plot of graphite/epoxy column CU43.

In this plot each point is the result of a single impact, and it represents the maximum magnitude of bending strain versus the maximum compressive strain recorded during this impact. The overall bending compression curve describes the dynamic flexure-compression behavior of the column, and it is employed for determination of the dynamic buckling strain (ϵ_{cr_d}). Dynamic buckling occurs when a small increase in axial compression due to a dynamic load results in a relatively large increase in the bending response. The Dynamic Load amplification Factor (DFL) for the column is calculated by the ratio

$$DLF = \frac{\epsilon_{cr_d}}{\epsilon_{cr_E}} \qquad (2)$$

where ϵ_{cr_E} is the static Euler buckling strain:

$$\epsilon_{cr_E} = \left(\frac{\pi}{\lambda_{eff}}\right)^2 \qquad (3)$$

and the effective slenderness ratio of the clamped column is:

$$\lambda_{eff} = \frac{L_{eff}}{r} = \frac{L}{2r} \quad . \qquad (4)$$

Since the duration of impulse (T) has an important influence on the dynamic buckling results, it should be specified for every column. It was shown in previous studies[1-3] that the nondimensional parameter

$$\tau = \frac{cT}{2L} \quad , \tag{5}$$

where

$$c = \frac{A_{11}}{\rho t} \tag{6}$$

is the longitudinal wave propagation velocity, is the appropriate representation of the duration of loading. In a test, τ is determined by the mass ratio of the striking mass (M) to the specimen (m) and is given by the approximate relation

$$\tau \simeq \frac{\pi}{2}\sqrt{\frac{M}{m}} \quad . \tag{7}$$

Note that τ is the number of times the stress wave front travels back and forth along the column during the duration of the impact.

In all the specimens the dynamic buckling was elastic. Their bending-compression plots, presented in[7] yielded quite definite values for the dynamic buckling strain, except several "shear" (S) laminates, where the curves bent up more gradually, making precise definition of buckling strain rather difficult.

In nine composite specimens (series -- 21) and in the aluminum alloy columns the impact testing was continued beyond buckling till failure, in order to observe the postbuckling behavior and the failure modes of the various materials.

Tests on nine different composite specimens (of the -- 22 series) were stopped immediately after initiation of buckling and they were sent to Dornier GmbH for ultrasonic and X-ray retesting after dynamic buckling. No material damage was observed. These specimens were then returned to the Technion and the impact tests were repeated. In general, the dynamic buckling results obtained were within the regular experimental scatter.

Moreover, nine additional different composite specimens were arbitrarily chosen for repeated dynamic buckling tests. In their first tests these columns were impacted at velocities significantly exceeding those for dynamic buckling. The only prerequisite for this retesting was that the specimens chosen should be visually undamaged. Even for these columns the repeated dynamic buckling results were within acceptable scatter.

The dynamic buckling results, including the repeated buckling tests which were performed about a year after the original tests are summarized in Tables 3 and 4 for the composite and aluminum alloy columns, respectively. In these Tables is an average of the results of Eqs. (5) and (7) and the number of passes of the wave front counted directly in the experimental record of the axial strain.

As in the previous studies[1-4] the results, when presented on a logarithmic scale of the DLF versus the slenderness ratio, result in straight lines, a line for each nondimensional duration of impulse, (see, for example, Fig. 2).

TABLE 3 - DYNAMIC BUCKLING RESULTS OF COMPOSITE COLUMNS

Spec. No.	λ_{eff}	τ	DLF	DLF (Southwell)	$\alpha\varepsilon_{b_o} 10^2$
CU11	53	7.8	1.3	1.5	22.0
		6.7	1.2	1.5	8.00
CU12		10.0	1.3	1.7	9.52
CU13		13.6	1.2	1.3	17.2
CU21	88	6.1	2.3	3.1	8.57
CU22		6.2	2.2	2.9	12.0
		6.7	2.7		
CU23		5.1	>3.6		13.7
CU31	132	6.4	4.6	7.2	15.6
CU32		5.5	5.8	8.5	14.5
CU33		4.2	7.2	7.9	16.5
CU41	197	6.4	7.9	10.0	10.0
CU42		3.8	12.6	15.0	12.8
CU43		4.7	10.2	12.4	15.4
CU51	285	6.0	13.1	17.2	26.2
		6.0	12.4		
CU52		5.1	11.1	17.6	18.5
CU53		3.9	17.2	25.4	12.2
CS11	50	9.6	1.3	1.5	8.40
CS12		12.5	1.2	1.9	16.7
CS13		7.5	2.1	2.3	10.1
CS21	83	6.2	3.9	5.0	8.82
CS22		6.2	1.9	2.7	13.7
		6.6	3.1		
CS23		4.9	2.7	5.7	25.6
CS31	125	6.1	4.0	6.3	18.3
		6.0	4.6		
CS32		5.3	4.0	6.5	26.3
CS33		4.4	4.3	8.5	15.2
CS41	188	6.4	6.3	11.1	17.5
CS42		4.6	12.2	16.3	17.2
CS43		4.0	13.3	18.1	16.7

TABLE 3 - (CONTINUED)

Spec. No.	λ_{eff}	τ	DLF	DLF (Southwell)	$\alpha\varepsilon_{b_o}$ 10^2
CS51	271	6.3	7.1	12.7	50.0
CS52		5.2	8.6	13.8	23.3
CS53		4.0	16.4	29.5	35.1
CM11	48	10.4	1.3	1.9	5.00
CM12		8.1	0.83	1.5	10.3
CM13		12.8	0.79	1.2	7.50
CM21	81	6.5	2.5	4.2	15.8
CM22		6.2	2.7	3.4	9.62
		6.9	2.7		
CM23		5.2	3.8	4.9	12.0
CM31	121	6.3	4.0	5.4	10.0
CM32		5.5	5.3	7.6	15.4
CM33		4.3	6.3	7.9	15.4
CM41	181	6.5	7.3	10.6	8.57
CM42		4.6	13.3	16.8	16.3
CM43		4.1	10.0	19.1	17.2
		4.0	10.6		
CM51	262	6.2	10.8	18.1	25.0
CM52		5.1	13.9	16.3	15.6
CM53		4.2	18.4	22.9	12.5
GU21	82	6.0	3.3	4.5	10.3
GU22		6.0	2.2	2.9	13.3
		6.2	2.0		
GU23		5.1	2.7	3.3	16.0
GU41	184	6.1	8.2	9.4	17.5
		3.3	9.9	11.6	
GU42		4.5	8.7	12.7	12.1
GU43		4.9	7.9	12.3	28.2
		5.0	8.2		
GS21	77	6.3	2.0	4.5	26.8
GS22		6.1	2.1	5.1	25.0
		6.1	2.2		

TABLE 3 - (CONTINUED)

Spec. No.	λ_{eff}	τ	DLF	DLF (Southwell)	$\alpha\varepsilon_{b_o}$ 10^2
GS23		4.6	2.1	3.6	12.0
		4.8	2.0		
GS41	173	6.4	3.8	5.0	33.1
		3.5	11.4	13.5	
GS42		4.5	7.7	13.3	30.8
GS43		6.2	4.5	9.2	16.8
GM21	77	6.0	3.1	4.0	8.33
GM22		5.7	3.1	3.7	11.5
		6.2	2.6		
GM23		4.6	3.2	3.8	17.1
		4.9	2.2		
GM41	173	6.0	7.6	9.5	11.5
		3.2	11.7	15.6	
GM42		4.5	10.0	13.2	24.6
GM43		4.9	8.3	10.6	23.8
KU21	104	6.4	2.3	4.6	11.0
KU22		6.4	2.7	3.5	7.69
		6.8	2.5		
KU23		4.7	2.7	4.0	11.0
KU41	234	6.5	6.1	11.9	7.50
		3.4	13.6	22.5	
KU42		4.8	7.2	11.7	34.5
		5.3	6.1		
KU43		3.8	9.7	18.9	13.6
KS21	91	6.4	4.4	5.5	9.09
KS22		6.4	4.0	5.0	7.78
		6.4	2.6		
KS23		4.6	2.8	5.5	18.2
KS41	205	6.5	5.1	10.2	14.1
		3.5	10.6	16.6	
KS42		5.4	4.3	7.9	34.1
KS43		4.2	8.1	12.8	21.4
		4.0	9.8		

TABLE 3 - (CONTINUED)

Spec. No.	λ_{eff}	τ	DLF	DLF (Southwell)	$\alpha\varepsilon_{b_o}$ 10^2
KM21	78	6.2	2.0	2.8	7.87
KM22		5.8	3.1	3.8	13.5
		6.2	1.5		
KM23		4.7	1.8	3.0	14.0
		4.8	2.2		
KM41	176	6.5	4.7	7.5	6.84
		3.4	9.7	13.0	
KM42		5.5	3.1	8.6	25.4
KM43		3.9	9.7	13.2	12.2

TABLE 4 - DYNAMIC BUCKLING RESULTS OF ALUMINUM ALLOY (2024-T3) COLUMNS

Specimen No.	λ_{eff}	τ	DFL
A31	249	6.0	6.0
		5.0	10.1
A32	108	6.5	3.0
A33	249	3.5	15.7
A34	206	5.5	9.0
A35	281	3.0	18.4
A36	206	3.0	14.6
A37	141	3.0	6.9
A38	141	5.4	5.1
A39	108	4.0	2.6
		3.4	3.3
A40	76	5.3	2.2
A41	76	5.0	2.2
A42	281	5.5	10.0

IV. Dicussion of Test Results

The results for the 2024-T3 aluminum alloy specimens (Table 4) are compared in Fig. 2 with previous results[1] for 6061-T4 aluminum alloy and AISI-01 steel specimens. Though the trend of the present results appears to be slightly different, the agreement is considered good since the experimental results are within the scatter of the results of[1]. This agreement

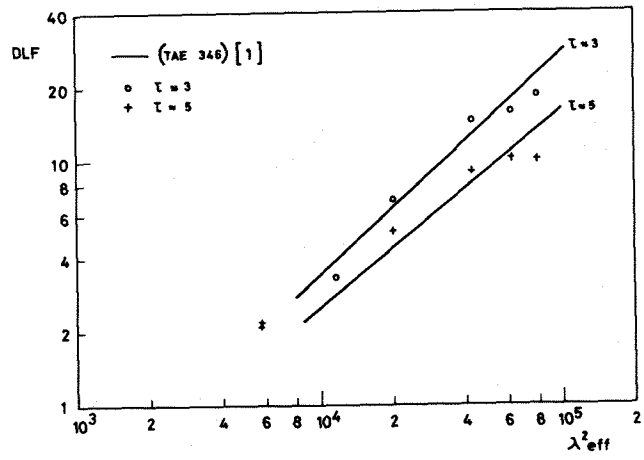

Figure 2. Results for metal specimens compared with (1).

for metal columns is clearly apparent in Figs. 3 and 4 where the corresponding results for the composite material and 2024-T3 aluminum alloy specimens are combined with those of[1].

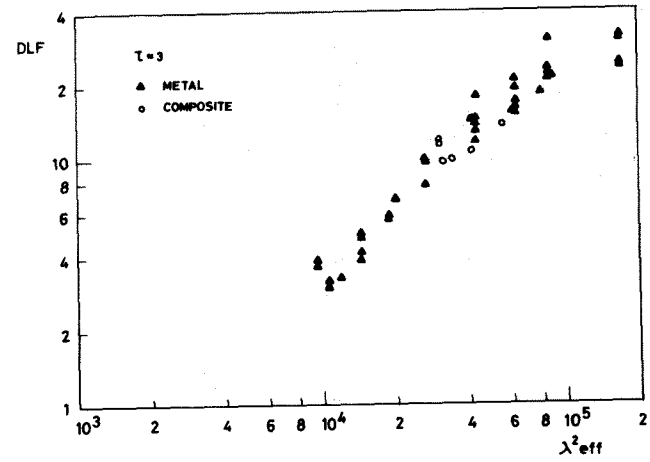

Figure 3. Combined results for $\tau \sim 3$.

A study of Fig. 4 raises the question why the scatter of the composite results is so large compared to that of the metals columns. One should remember that the metal specimens are of AISI-01 steel, 6061-T4 and 2024-T3 aluminum alloys. The answer to this question requires some insight into the behavior of the various composite laminates.

Though three composite materials were employed for the manufacture of the specimens, most of the columns were of graphite/epoxy. The results of DLF versus slenderness ratio for this material are presented in Figs. 5, 6 and 7 for the unidirectional (CU), "shear" (CS) and "mixed" (CM) laminates, respectively. It is immediately seen that the results for the CU and CM specimens are within narrow bands of scatter,

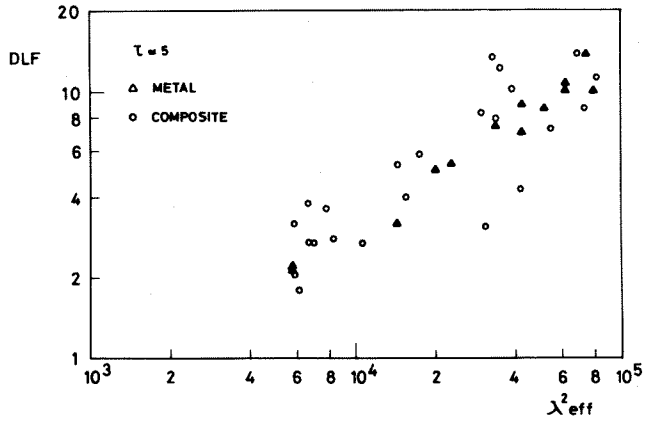

Figure 4. Combined results for $\tau \sim 5$.

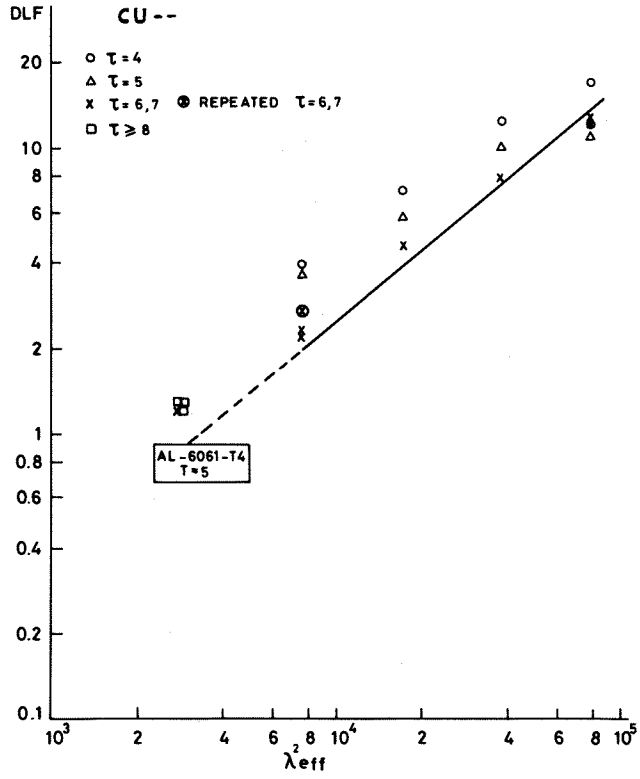

Figure 5. Results for unidirectional graphite/epoxy columns.

whereas the scatter of results in Fig. 6 for the "shear" laminates is relatively large. The exceptional behavior of the CS layup is emphasized in Fig. 8 where the narrow scatter observed for the CU and CM laminates is disturbed by several anomalous CS results. This conclusion is not restricted to the graphite/epoxy (C) columns. A significant scatter also appears for "shear" laminated Kevlar/epoxy (KS) columns.

The conclusion that unidirectional and "mixed" layups provide more consistent dynamic buckling results, may be complemented by the conclusion that Kevlar/epoxy columns yield lower dynamic buckling strains than graphite/epoxy and

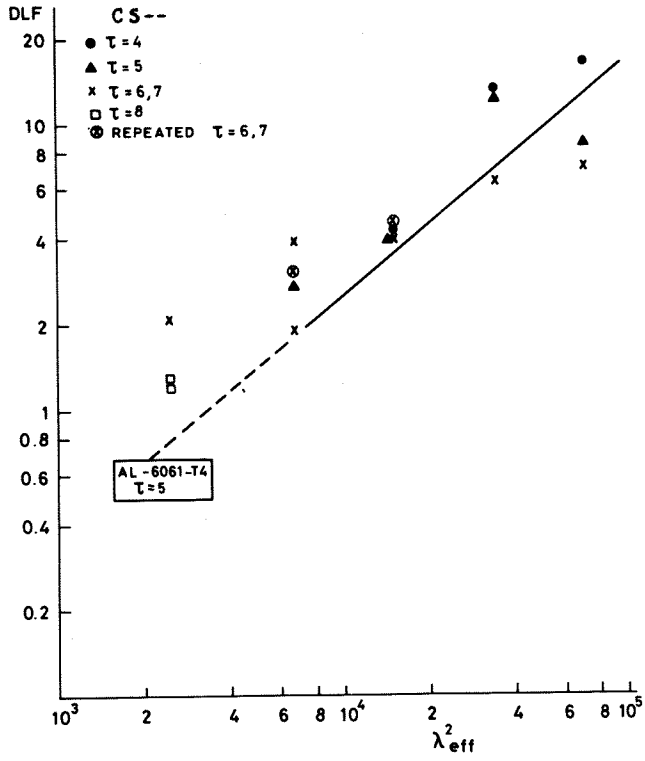

Figure 6. Results for "shear" graphite/epoxy columns.

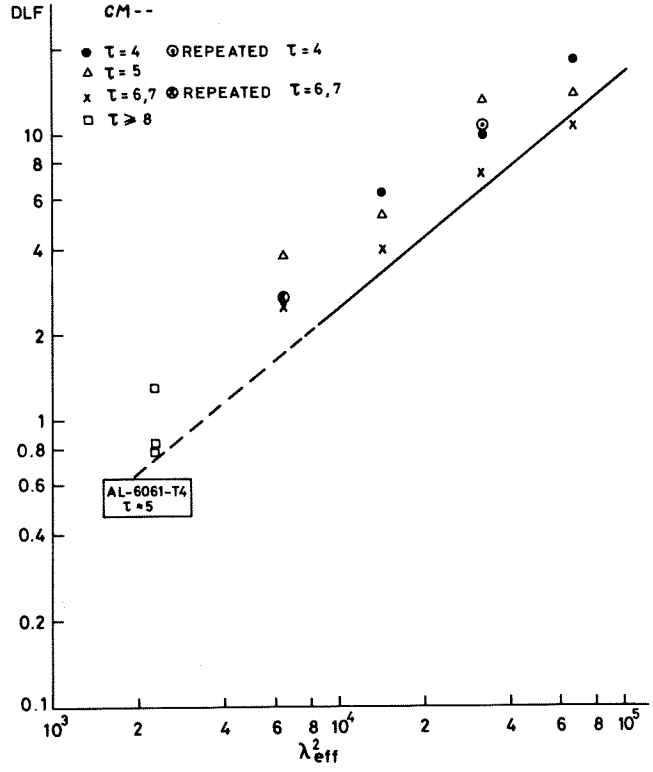

Figure 7. Results for "mixed" graphite/expoxy columns.

glass/epoxy columns (also shown in Figs. 14 and 15 of[7]).

In Section 2, test results of the static elastic properties were compared with the predicted ones. It was stated there that,

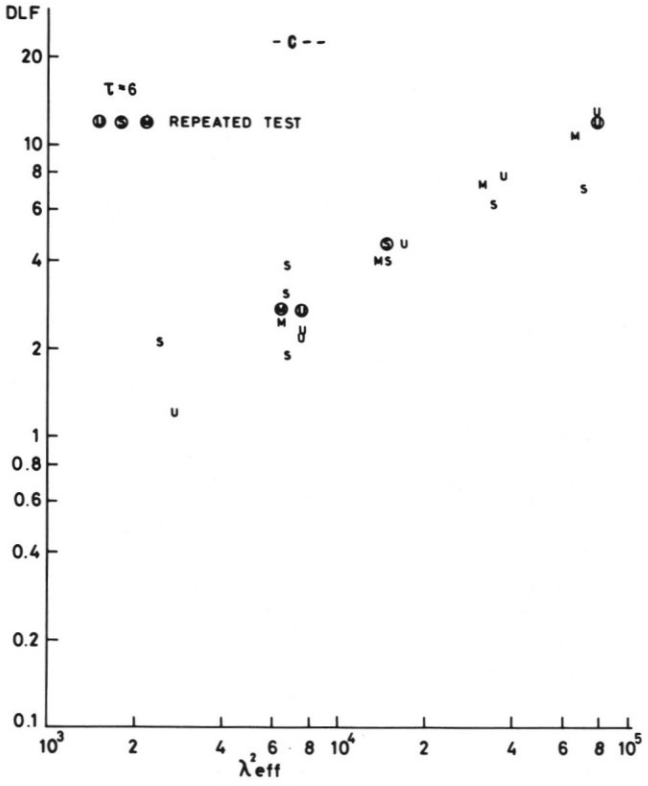

Figure 8. Results for graphite/expoxy columns. ($\tau \sim 6$).

except in the glass/epoxy specimens, the actual measured properties of the "shear" laminates were appreciably lower than the predicted ones. It was also found that the properties of all the Kevlar/epoxy laminates were much below the computed ones. Hence, as in the case of the static stiffness properties, the dynamic buckling behavior is possibly affected by poor composite material quality caused by weak fiber-matrix bonding and inefficient shear transfer.

A summary of the dynamic buckling results according to the classification of relatively poor composite material quality and relatively high material quality is presented in Fig. 9. Glass-fiber and graphite fiber laminates (except CS), for which good agreement was observed between static stiffness test results and predicted stiffnesses, have superior dynamic buckling properties, which exceed those of the metal columns. On the other hand, poor agreement between predicted and tested static stiffness properties leads to relatively low DLF's. The advantage of the high quality composite material over the metal columns can therefore be attributed mainly to their almost perfect elastic behaviour and flatness of the specimens.

The major disadvantage of the glass/epoxy and graphite/epoxy laminates is the fracture of material in the post buckling region. Whereas

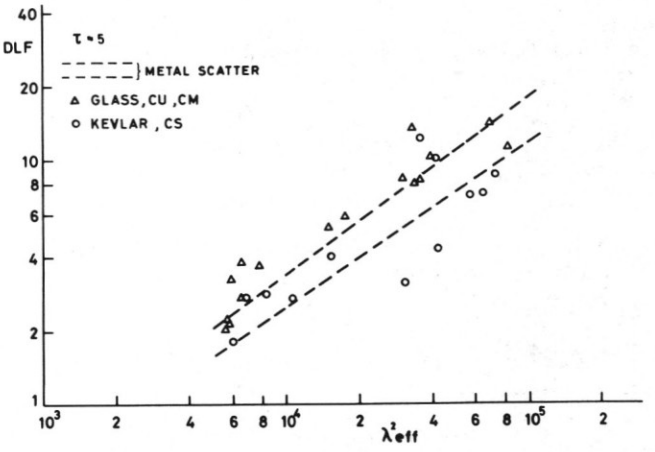

Figure 9. Classification of composite material columns into two categories for dynamic buckling.

Kevlar/epoxy specimens have high energy absorption capability and metal columns suffer plastic deformations, the superior composite materials (glass and graphite/epoxy) fail by delamination or tearing or by a combination of both modes (see Fig. 10). The weak bond between

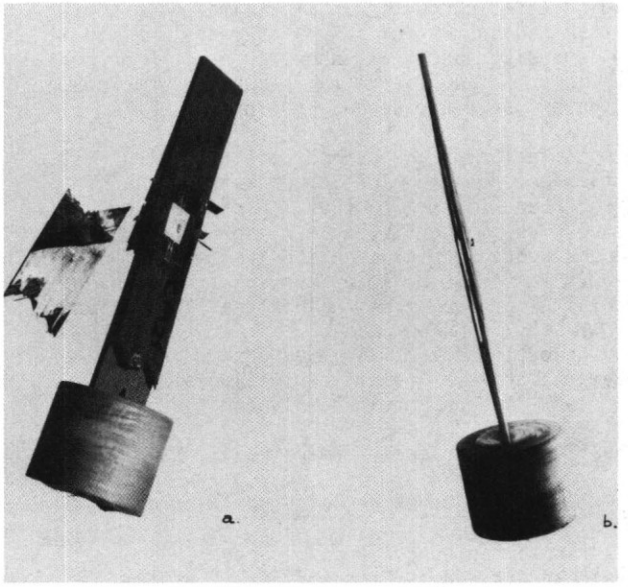

Figure 10. Fracture modes of (a) graphite/epoxy column CM21 and (b) glass/epoxy column GM21.

the Kevlar fiber and the epoxy matrix, that was considered a disadvantage when initial dynamic buckling was studied, apparently becomes an advantage for post buckling resistance of the impacted column.

Dynamic buckling of columns is sensitive to initial geometrical imperfection. In[2] a "generalized Southwell equation" which yields an extension to the well-known Southwell method (see, for example[9] or [10]) was presented as follows:

$$\frac{\Delta w}{\varepsilon_c} = w_o\left(\alpha + \frac{\beta}{\varepsilon_{cr}^2}\right) + \frac{1}{\varepsilon_{cr}}\left(\alpha w - \alpha w_o \varepsilon_c\right) \qquad (8)$$

where α and β are coefficients, w_o is the initial geometrical imperfection, ε_c is the compressive strain which causes a deflection Δw and ε_{cr} is the buckling strain defined here by the upper bound of ε_c as follows:

$$\varepsilon_{cr} = \lim_{\Delta w \to \infty} \varepsilon_c \qquad (9)$$

Eq. (8) can be rewritten as

$$\frac{\varepsilon_b}{\varepsilon_c} = \varepsilon_{b_o}\left(\alpha + \frac{\beta}{\varepsilon_{cr}^2}\right) + \frac{1}{\varepsilon_{cr}}\left(\varepsilon_b - \alpha\varepsilon_{b_o}\varepsilon_c\right) \qquad (10)$$

where ε_{b_o} is the strain that represents the initial geometrical imperfection of the column. The term $\varepsilon_{b_o}\left(\alpha + \beta/\varepsilon_{cr}^2\right)$ is constant, and a plot of $\varepsilon_b - \alpha\varepsilon_{b_o}\varepsilon_c$ versus $(\varepsilon_b/\varepsilon_c)$ would, therefore, yield a straight line, whose slope is ε_{cr}. This method provides a well defined criterion for dynamic buckling, but it yields upper bounds which significantly exceed the dynamic buckling strains obtained from the experiments. Since the generalized Southwell method, as its original static counterpart, is limited to the elastic region, it can be reliably applied for the composite specimens, whereas for the metal specimens its applicability is confined to the region of large slenderness ratios.

Application of the method to a typical bending-compression plot is demonstrated in Fig. 11 together with the Southwell plot obtained. The results, listed in Table 3, do not change the observations discussed and the conclusions drawn. It should be noted, however, that the initial slope $(\alpha\varepsilon_{b_o})$ of the bending compression may indicate the initial imperfection of the column. Large values of the initial slope $(\alpha\varepsilon_{b_o} > 0.3)$ were obtained only for several "shear" or Kevlar/epoxy laminates.

V. Theoretical Studies

A finite difference computer code IMPCOL developed earlier at Technion([2] and [11]) was used to compute the response of the columns. For some columns calculations were also carried out with the dynamic part of the finite element code COSA developed by Dornier[12]. As in the experiments, the loading of the column in IMPCOL results from a collision with a moving mass. In COSA, however, the loading is represented by a half sine time dependent axial compression.

A comparison of test results for graphite/epoxy unidirectional (CU) specimens with numerical results obtained with IMPCOL is shown in Fig. 12. The experimental DLF's in the figure were obtained by the "generalized Southwell method". It was found in[2] that

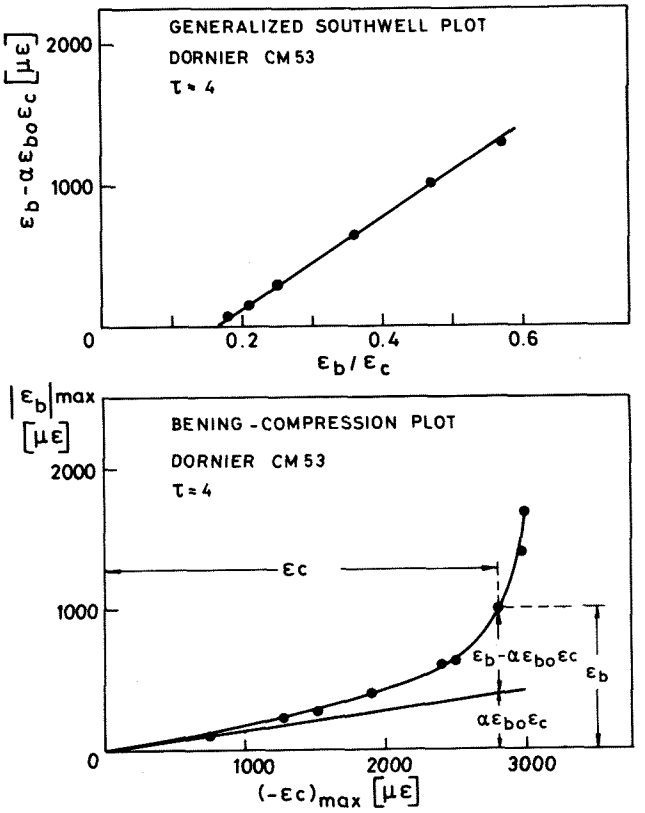

Figure 11. "Generalized Southwell plot" derived from bending-compression plot.

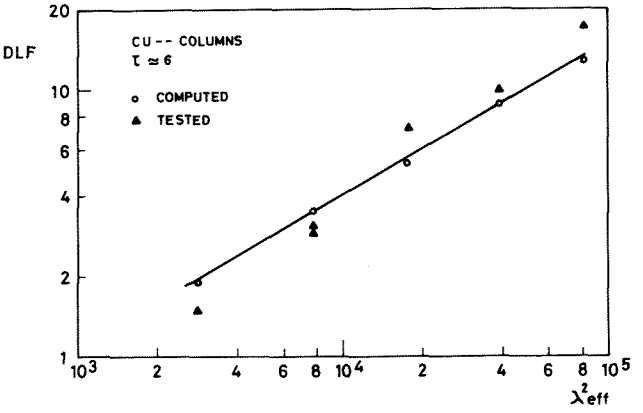

Figure 12. Comparison of computed and tested "generalized Southwell" results.

the test rig employed in the experiments contributes an equivalent imperfection of amplitude $w_o \tilde{} 0.6$ mm, and this magnitude of imperfection was also attributed to the columns computed here. The agreement between the numerical and experimental results in Fig. 12 is fairly good, although the slope of the calculated line on the log - log plot is slightly less than the general trend of the test results.

Figure 13 shows a bending-compression plot

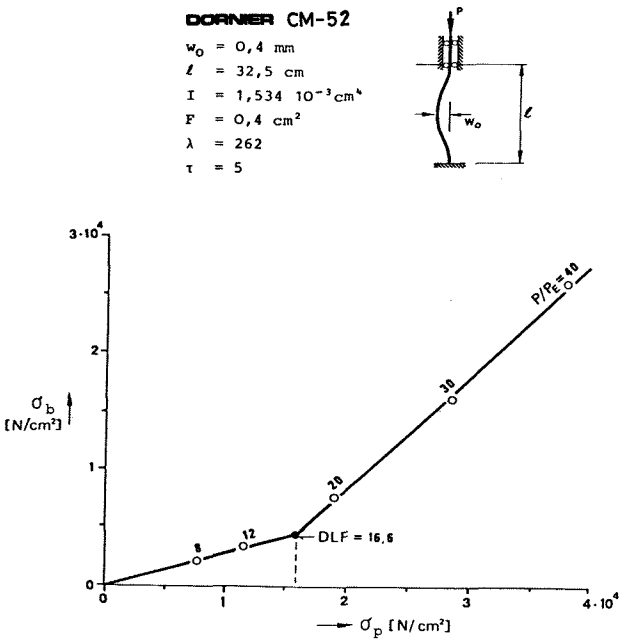

Figure 13. Bending-compression plot for graphite/epoxy specimen CM52 computed with COSA.

computed with COSA for column CM52. The computed DLF of 16.6 agrees very well with the test result of 16.3 obtained by the "generalized Southwell method" (see Table 3).

Since both computer codes assume an elastic material and differentiate between materials only by their stiffness, the numerical results cannot include all the effects of material properties. One exception was a numerical study of material damping carried out with IMPCOL, in which the damping coefficients were varied in a wide range, much beyond practical magnitudes, but the differences in dynamic buckling strains observed were insignificant.

VI. Conclusions

1. The Dynamic Load amplification Factors (DLF) of composite material columns are usually higher than those of corresponding metal columns.
2. Composite laminates whose elastic coefficients are much lower than the predicted ones have also inferior dynamic buckling properties. A possible explanation may be the deviation of the quality of fiber-matrix bond from the assumption of perfect bonding.
3. "Shear" laminates (±45°) have the lowest dynamic buckling resistance. This disadvantage is pronounced in Kevlar/epoxy laminates that have the weakest fiber-matrix bond, is significant in graphite/epoxy columns, and is noticeable even in the results for glass/epoxy specimens (with the apparently strongest fiber-matrix bond).
4. "Mixed" (quasi-isotropic) and unidirectional laminates, which both have longitudinal filaments in the outer laminae, yield the highest DLF's (except for the Kevlar specimens).
5. The "best" average dynamic buckling results were obtained for the glass/epoxy laminates and the lowest for the Kevlar/epoxy ones. However, if the "shear" graphite/epoxy laminates are not considered, this material can be graded the "best", since the DLF's for the CU and CM columns are higher than those for the GU and GM ones.
6. The postbuckling resistance of the Kevlar/epoxy material is better than that of the other two composites. It is anticipated therefore that hybrid laminates with longitudinal graphite or glass-fibers in the outer laminae and Kevlar on the inside will combine their properties to yield the "best" dynamic buckling and post buckling behavior.
7. Large differences in the material damping properties have only a minor effect on dynamic buckling in the elastic range.
8. The wide elastic region of the fibers in composite materials permits the application of a "generalized Southwell method" for the determination of the dynamic buckling load.
9. Initiation of dynamic buckling does not cause damage in the material that can be detected by ultrasonic or X-ray tests. Repeated dynamic buckling tests on composite columns yielded results generally similar to those of the first tests. Hence, the composite material columns may withstand repeated dynamic buckling, provided that dynamic buckling loads are not significantly exceeded (to prevent the possibility of fracture). It may be pointed out that the results of the repeated tests were not influenced by the long period between tests, indicating no significant material deterioration.
10. Good agreement is found between experimental DLF's obtained with the "generalized Southwell method" and the DLF's computed with a finite difference program IMPCOL or with a finite element program COSA.

Acknowledgements

The authors wish to express their gratitude to Mr. S. Nachmani, Mr. A. Grunwald, Mr. G. Rubin and Mr. M. Kollet for their devoted assistance during all stages of the research. They also wish to thank Mrs. A. Goodman-Pinto for the typing of the manuscript and Mrs. I. Nitzan for the preparation of the figures.

References

1. Ari-Gur, J., Weller, T. and Singer, J., "Experimental Studies of Columns under Axial Impact", TAE Report 346, Dept. of Aeronautical Engineering, Technion-Israel Inst. of Technology, Haifa, Israel, December 1978.

2. Ari-Gur, J., Weller, T. and Singer, J., "Theoretical Studies of Columns under Axial Impact and Experimental Verification", TAE Report No. 377, Dept. of Aeronautical Engineering, Technion-Israel Inst. of Technology, Haifa, Israel, August 1979.

3. Ari-Gur, J., "Stability of Thin Laminated Structures under Impulsive Compression", D.Sc. Thesis (in Hebrew), Dept. of

Aeronautical Engineering, Technion-Israel Inst. of Technology, Haifa, Israel, May 1980.

4. Ari-Gur, J., Weller, T. and Singer, J., "Experimental and Theoretical Studies of Column under Axial Impact", International Journal of Solids and Structures (to be published).

5. Ari-Gur, G., "Dynamically Self-Supported Columns", (to be published).

6. Singer, J. and Ari-Gur, J., "Dynamic Buckling of Thin-Walled Structures under Impact", DGLR Annual Meeting, RWTH, Aachen, Germany, (Paper No. 81-077), May 1981.

7. Ari-Gur, J. and Singer, J., "Composite Material Columns under Axial Impact", TAE Report 462, Dept. of Aeronautical Engineering, Technion-Israel Inst. of Technology, Haifa, Israel, December 1981.

8. Röhrle, H., "Bestimmung des Dynamischen Beulverhaltens von Stäben aus Faserverbundwerkstoffen bei Stossformigen Lasten", Zwischenbericht, Dornier GmbH Bericht Nr. SB-20-8009/01, September 1980.

9. Southwell, R.V., "On the Analysis of Experimental Observations in Problems of Elastic Stability", Proceedings Royal Society, London, Series A, Vol. 135, pp. 601-616.

10. Timoshenko, S.P. and Gere, J.M., Theory of Elastic Stability, 2nd Ed., McGraw Hill, New York, 1961.

11. Ari-Gur, J., "IMCOL (extended) - Program for Imperfect Composite Column with Damping under Axial Impact", ASL Report No. 114 Aircraft Structures Laboratory, Dept. of Aeronautical Engineering, Technion-Israel Inst. of Technology, Haifa, Israel, February 1981.

12. COSA-DYNAME System, Dornier GmbH, Friedrichshafen, 1974.

Appendix - Notation

A_{11}	elastic coefficient of longitudinal stiffness
b	width of specimen
c	velocity of longitudinal wave propagation, Eq. (6)
D_{11}	elastic coefficient of bending stiffness
DLF	dynamic load amplification factor, Eq. (2)
L	length of column
M	striking mass
m	mass of column
r	radius of gyration of cross-section, Eq. (1)
T	duration of impulse
t	thickness of column
w	deflection from axis
w_o	initial geometrical imperfection
α	coefficient, Eq. (8)
β	coefficient, Eq. (8)
Δw	deflection = $w - w_o$
ε_b	bending strain
ε_{b_o}	initial bending strain
ε_c	axial strain
ε_{cr_d}	dynamic buckling strain
ε_{cr_E}	static Euler buckling strain, Eq. (3)
λ_{eff}	effective slenderness ratio, Eq. (4)
ρ	mass density
τ	nondimensional duration of impulse, Eq. (5)